Maneuver Algorithm for Mobile Robot with Four Steered Propulsive Wheels

HE XU[1,2], WEI DA WANG[2] AND MARIE BERNARD SIDIBE[2]
School of Mechanics and Electronics Engineering
1. Harbin Engineering University,245-11 Nantong Street, Nangang District, Harbin 150001, CHINA
2. Harbin Institute of Technology,92 Xidazhi Street, Nangang District, Harbin 150001, CHINA

Abstract: - The algorithm formula in explicit format for the maneuver of wheeled mobile robot (WMR) with four steered independently driven wheels (4WS4WD) is rarely discussed. Based on the constraints of pure rolling and non slip, the existence of ICR (Instantaneous Center of Rotation) has been proofed toward this class of robots. A generic maneuver algorithm based on ICR (including the direction of rotation) has been presented in explicit format. And a generic maneuver algorithm with constraints has also been investigated explicitly to limit the orientation range of steering wheels. Several typical maneuver modes with rotation direction have been drawn from the generic maneuver algorithm mentioned above. Results from simulation and tests are presented to demonstrate the feasibility of proposed algorithms.

Key-Words: - mobile robot, generic maneuver algorithm, instantaneous center of rotation

1 Introduction

The maneuver features of a WMR are very important in the domain of its application. A WMR with 4WS4WD is a redundantly actuated robot under the constraints of pure rolling on horizontal plane. The explicit maneuver algorithms about this class of robot mentioned above are rarely discussed though several similar literatures are available.

B.C. Besselink proposed a non-conflicting secondary steering algorithm on vehicles with two independently driven wheels and gives a control diagram about the maneuver control strategy [1]. Thomas Bak presented a mobility control algorithm to a robotic platform used in agriculture by decoupling adjustments in position from adjustments in orientation [2]. Thomas Bak also gave control algorithm to a mobile robotic platform by using hybrid control strategy to a nonlinear trajectory tracking issue. The singular points in configuration space had been discussed [3]. To a four-driven and four-steered mobile robot, a kind of practical maneuver algorithm in explicit format is really needed in the process of control. Thus a research focused the generic maneuver control algorithm has been carried by our research group.

In this paper, the features of the mobile robot are introduced in section 2. The proof of existence of ICR has been presented in section 3. A generic maneuver algorithm is derived in section 4. A generic maneuver algorithm with constraints is given in section 5. Test results have been implemented in section 6. Conclusions and future work are proposed in section 7.

2 Robot Features

The Fig.1 is robot platform with reconfigurable chassis and caster angles and the chamber angles of wheels. The differential device makes four wheels of robot contact the terrain and average load to the four wheels. Further more, a less pitch of robot body will be available when robot travels in rough terrain. The robot has the potential ability to perform diversified steering modes, such as Omni-directional mode, Ackerman mode, Double-Ackerman mode, Point-turn mode, etc.

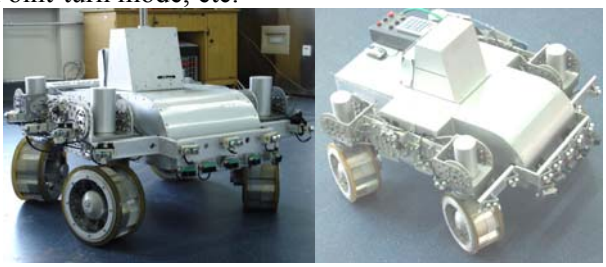

Fig.1 Mobile robot with 4WS4WD

3 Existence of ICR

Hypothesis: The robot is in horizontal plane with four rigid driven wheels and rigid frame. The wheels can steer around their vertical axles. The wheels contact with ground at a point with pure rolling.

Theorem: The motion of a robot with 4WS4WD in a plane under the assumption above can be described as a rotation motion around ICR and a translation motion (in this case, the ICR can be regarded as being at infinity), i.e. there always exists an ICR at any instantaneousness.

Proof: As shown in Fig.2, L and W are the length and width of the robot frame. $\gamma_0 = \text{atan}(W/L)$; $p = 0.5\sqrt{W^2 + L^2}$ The main kinematic parameters of WMR are in Table 1.

Table 1. Kinematics Parameters of Mobile Robot

Wheels	α(rad)	β (rad)	l (m)
1c	γ_0	β_1	p
2c	2π - γ 2π - γ_0	$\beta_1\beta_1\beta_1$ β_2	p
3c	π - γ_0	β_3	p
4c	$\pi + \gamma_0$	β_4	p

The kinematic constraints of the robot can be written as follows:

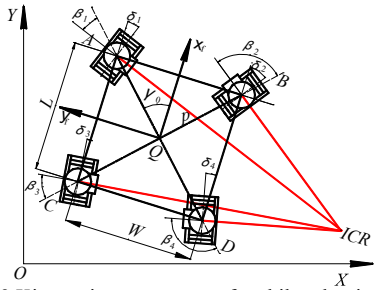

Fig.2 Kinematics parameters of mobile robot in coordinate.

$$C_1(\beta_s)R(\theta)\dot{\xi} = 0 \tag{1}$$

Where the rotation matrix $R(\theta) = \begin{bmatrix} \cos\theta & \sin\theta & 0 \\ -\sin\theta & \cos\theta & 0 \\ 0 & 0 & 1 \end{bmatrix}$

The position and orientation variable $\xi = (x, y, \theta)^{\mathrm{T}}$

$$C_1(\beta_s) = \begin{bmatrix} \cos(\gamma_0 + \beta_1) & \sin(\gamma_0 + \beta_1) & p\sin\beta_1 \\ \cos(\pi - \gamma_0 + \beta_3) & \sin(\pi - \gamma_0 + \beta_3) & p\sin\beta_3 \\ \cos(2\pi - \gamma_0 + \beta_2) & \sin(2\pi - \gamma_0 + \beta_2) & p\sin\beta_2 \\ \cos(\pi + \gamma_0 + \beta_4) & \sin(\pi + \gamma_0 + \beta_4) & p\sin\beta_4 \end{bmatrix} \tag{2}$$

As $\beta_1 = \pi/2 + \delta_1 - \gamma_0$; $\beta_3 = -\pi/2 + \delta_3 + \gamma_0$;
$\beta_2 = \pi/2 + \delta_2 + \gamma_0$; $\beta_4 = -\pi/2 + \delta_4 - \gamma_0$;

So $$C_1(\beta_s) = \begin{bmatrix} -\sin\delta_1 & \cos\delta_1 & p\cos(\delta_1 - \gamma_0) \\ -\sin\delta_2 & \cos\delta_2 & p\cos(\delta_2 + \gamma_0) \\ -\sin\delta_3 & \cos\delta_3 & -p\cos(\delta_3 + \gamma_0) \\ -\sin\delta_4 & \cos\delta_4 & -p\cos(\delta_4 - \gamma_0) \end{bmatrix} \tag{3}$$

As $$R(\theta)\dot{\xi} \in Ker[C_1(\beta_s)]$$

For vector $\forall n = R(\theta)\dot{\xi} \in Ker[C_1(\beta_s)]$, it always satisfies the coupled equations $C_1(\beta_s)n = 0$. The ample and essential condition of the existence of non-trivial solutions for these homogeneous coupled equations is as follows:

$$rank[C_1(\beta_s)] \le 2 \tag{4}$$

A zero motion line [4] is a line through the horizontal axis of a wheel, perpendicular to the wheel plane. In coordinate in Fig.2, the four *zero motion lines* are described by the following equations.

$$x\cos\delta_1 + y\sin\delta_1 = p\cos(\delta_1 - \gamma_0) \tag{5}$$
$$x\cos\delta_2 + y\sin\delta_2 = p\cos(\delta_2 + \gamma_0) \tag{6}$$
$$x\cos\delta_3 + y\sin\delta_3 = -p\cos(\delta_3 + \gamma_0) \tag{7}$$
$$x\cos\delta_4 + y\sin\delta_4 = -p\cos(\delta_4 - \gamma_0) \tag{8}$$

It can be written in matrix form:

$$AX = B \tag{9}$$

The coefficients matrix:

$$A = \begin{bmatrix} \cos\delta_1 & \sin\delta_1 \\ \cos\delta_2 & \sin\delta_2 \\ \cos\delta_3 & \sin\delta_3 \\ \cos\delta_4 & \sin\delta_4 \end{bmatrix} \tag{10}$$

The expended matrix:

$$A_b = \begin{bmatrix} \cos\delta_1 & \sin\delta_1 & p\cos(\delta_1 - \gamma_0) \\ \cos\delta_2 & \sin\delta_2 & p\cos(\delta_2 + \gamma_0) \\ \cos\delta_3 & \sin\delta_3 & -p\cos(\delta_3 + \gamma_0) \\ \cos\delta_4 & \sin\delta_4 & -p\cos(\delta_4 - \gamma_0) \end{bmatrix} \tag{11}$$

To coupled equations (11), the ample and essential conditions of the existence of non-trivial solutions for this coupled equations is as

$$rank(A) = rank(A_b) \tag{12}$$

To $\forall\ \delta_i \in (-\pi, \pi]$, no δ_i can satisfy:

$$\cos\delta_i = \sin\delta_i = 0$$
$$\therefore\ \ 1 \le rank(A) \le 2 \tag{13}$$
$$1 \le rank(A_b) \tag{14}$$

After a primary transformation:

$$A_b \xrightarrow[-1\times Col_1]{Col_1 \text{ and } Col_2 \text{ interchange}} C_1(\beta_s)$$
$$rank(A_b) = rank(C_1(\beta_s)) \le 2$$
$$\therefore\ \ 1 \le rank(A_b) \le 2 \tag{15}$$

$$\overline{\Delta_1} = \begin{vmatrix} \cos\delta_1 & \sin\delta_1 & p\cos(\delta_1 - \gamma_0) \\ \cos\delta_2 & \sin\delta_2 & p\cos(\delta_2 + \gamma_0) \\ \cos\delta_3 & \sin\delta_3 & -p\cos(\delta_3 + \gamma_0) \end{vmatrix} = 0 \tag{16}$$

$$\overline{\Delta_2} = \begin{vmatrix} \cos\delta_1 & \sin\delta_1 & p\cos(\delta_1 - \gamma_0) \\ \cos\delta_2 & \sin\delta_2 & p\cos(\delta_2 + \gamma_0) \\ \cos\delta_4 & \sin\delta_4 & -p\cos(\delta_4 - \gamma_0) \end{vmatrix} = 0 \tag{17}$$

$$\overline{\Delta_3} = \begin{vmatrix} \cos\delta_2 & \sin\delta_2 & p\cos(\delta_2 + \gamma_0) \\ \cos\delta_3 & \sin\delta_3 & -p\cos(\delta_3 + \gamma_0) \\ \cos\delta_4 & \sin\delta_4 & -p\cos(\delta_4 - \gamma_0) \end{vmatrix} = 0 \tag{18}$$

$$\overline{\Delta_4} = \begin{vmatrix} \cos\delta_3 & \sin\delta_3 & -p\cos(\delta_3 + \gamma_0) \\ \cos\delta_4 & \sin\delta_4 & -p\cos(\delta_4 - \gamma_0) \\ \cos\delta_1 & \sin\delta_1 & p\cos(\delta_1 - \gamma_0) \end{vmatrix} = 0 \tag{19}$$

Where $\overline{\Delta_i}, (i = 1, \ldots, 4)$ is one of the 3rd order sub-determinates of matrix A_b.

1). **When** $rank(A) = 1$

The 2nd order sub-determinates of matrix A. are as

$$\Delta_1 = \begin{vmatrix} \cos\delta_1 & \sin\delta_1 \\ \cos\delta_2 & \sin\delta_2 \end{vmatrix} = 0 \quad (20)$$

$$\Delta_2 = \begin{vmatrix} \cos\delta_1 & \sin\delta_1 \\ \cos\delta_3 & \sin\delta_3 \end{vmatrix} = 0 \quad (21)$$

$$\Delta_3 = \begin{vmatrix} \cos\delta_1 & \sin\delta_1 \\ \cos\delta_4 & \sin\delta_4 \end{vmatrix} = 0 \quad (22)$$

$$\Delta_4 = \begin{vmatrix} \cos\delta_2 & \sin\delta_2 \\ \cos\delta_3 & \sin\delta_3 \end{vmatrix} = 0 \quad (23)$$

$$\Delta_5 = \begin{vmatrix} \cos\delta_2 & \sin\delta_2 \\ \cos\delta_4 & \sin\delta_4 \end{vmatrix} = 0 \quad (24)$$

$$\Delta_6 = \begin{vmatrix} \cos\delta_3 & \sin\delta_3 \\ \cos\delta_4 & \sin\delta_4 \end{vmatrix} = 0 \quad (25)$$

A solution can be achieved from (20) to (25):

$$\delta_1 = \delta_2 = \delta_3 = \delta_4 \quad (26)$$

To $\delta_i \in [-\pi, \pi]$; $(i = 1,2,3,4)$, as long as $\delta_i \neq 0, \pi$ or $\delta_i \neq \pm 0.5\pi, (i = 1,2,3,4)$ (In these cases the robot are degenerated to a bicycle with two wheels!), there must be at lest a non-zero 2nd order sub-determinates in matrix A_b.

$$\therefore \quad rank(A_b) = 2$$

$$rank(A) \neq rank(A_b) \quad (27)$$

There is no solution in the coupled equations (9). This situation presents an obvious geometrical meaning: the *zero motion lines* of the four wheels are parallel and have no intersect point. ICR can be regarded as being at infinity.

2). **When** $rank(A) = 2$

There must be a $\Delta_i \neq 0 \quad (i = 1,2,...,6)$,

$$\therefore \quad rank(A) = rank(A_b) = 2 \quad (28)$$

There are non-trivial solutions in the coupled equations (9). This situation presents an obvious geometrical meaning: *the zero motion lines* of the four wheels intersect at a common point, i.e. ICR exists. The relations of $\delta_1, \delta_2, \delta_3, \delta_4$ are described in (16) to (19).

4 Generic Maneuver Algorithm

The relations of control parameters of WMR with 4WS4WD are shown in Fig.3.

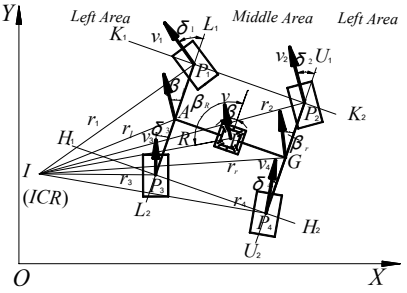

Fig.3 Relations among control parameters of robot

The steering angles of wheel are as follows:

$$\delta_i \in (-\pi, \pi]; \quad i = 1,2,3,4 \quad (29)$$

The position of ICR is described by the maneuver radius $R \in [0, \infty)$ and the azimuth $\beta_R \in (-\pi, -\pi]$. The following sets are defined to identify the position of ICR.

Let $M_+ = \{(R,\beta_R) \mid (-1)^d R\sin\beta_R + (-1)^{d+1} W/2 \geq 0\}$

$M_- = \{(R,\beta_R) \mid (-1)^d R\sin\beta_R + (-1)^{d+1} W/2 < 0\}$

$N_+ = \{(R,\beta_R) \mid (-1)^d R\sin\beta_R + (-1)^d W/2 \geq 0\}$

$N_- = \{(R,\beta_R) \mid (-1)^d R\sin\beta_R + (-1)^d W/2 < 0\}$

$P_+ = \{(R,\beta_R) \mid (-1)^d R\cos\beta_R + (-1)^{d+1} L/2 \geq 0\}$

$P_- = \{(R,\beta_R) \mid (-1)^d R\cos\beta_R + (-1)^{d+1} L/2 < 0\}$

$Q_+ = \{(R,\beta_R) \mid (-1)^d R\cos\beta_R + (-1)^d L/2 \geq 0\}$

$Q_- = \{(R,\beta_R) \mid (-1)^d R\cos\beta_R + (-1)^d L/2 < 0\}$

$S_1 = \{(R,\beta_R) \mid R = p, \beta_R = \gamma_0\}$

$S_3 = \{(R,\beta_R) \mid R = p, \beta_R = \pi - \gamma_0\}$

$S_2 = \{(R,\beta_R) \mid R = p, \beta_R = -\gamma_0\}$

$S_4 = \{(R,\beta_R) \mid R = p, \beta_R = -\pi + \gamma_0\}$

Where d is the rotation direction index, d=0 is for anti-clockwise and d=1 is for clockwise.

The radius of each wheel around ICR is as follows:

$$r_1 = \sqrt{R^2 + 0.25(W^2 + L^2) - RL\cos\beta_R - RW\sin\beta_R} \quad (30)$$

$$r_3 = \sqrt{R^2 + 0.25(W^2 + L^2) + RL\cos\beta_R - RW\sin\beta_R} \quad (31)$$

$$r_2 = \sqrt{R^2 + 0.25(W^2 + L^2) - RL\cos\beta_R + RW\sin\beta_R} \quad (32)$$

$$r_4 = \sqrt{R^2 + 0.25(W^2 + L^2) + RL\cos\beta_R + RW\sin\beta_R} \quad (33)$$

The steering angle of each wheel is as follows:

$$\delta_1 = \begin{cases} (-1)^d \arcsin[(0.5L - R\cos\beta_R)/r_1]; (R,\beta_R) \in M_+ \cap \overline{S_1} \\ \pi - (-1)^d \arcsin[(0.5L - R\cos\beta_R)/r_1]; (R,\beta_R) \in M_- \cup P_- \\ -\pi - (-1)^d \arcsin[(0.5L - R\cos\beta_R)/r_1]; (R,\beta_R) \in M_- \cup P_+ \\ 0; \quad (R,\beta_R) \in S_1, where\ \overline{S_1} is\ the\ \sup\ plementary\ set\ of\ S_1 \end{cases} \quad (34)$$

$$\delta_3 = \begin{cases} (-1)^d \arcsin[(-0.5L - R\cos\beta_R)/r_3]\ ; (R,\beta_R) \in M_+ \cap \overline{S_3} \\ \pi - (-1)^d \arcsin[(-0.5L - R\cos\beta_R)/r_3]\ ; (R,\beta_R) \in M_- \cup Q_- \\ -\pi - (-1)^d \arcsin[(-0.5L - R\cos\beta_R)/r_3]\ ; (R,\beta_R) \in M_- \cup Q_+ \\ 0\ ; \quad (R,\beta_R) \in S_3 where\ \overline{S_3} is\ the\ \sup\ plementary\ set\ of\ S_3 \end{cases} \quad (35)$$

$$\delta_2 = \begin{cases} (-1)^d \arcsin[(0.5L - R\cos\beta_R)/r_2]\ ; (R,\beta_R) \in N_+ \cap \overline{S_2} \\ \pi - (-1)^d \arcsin[(0.5L - R\cos\beta_R)/r_2]\ ; (R,\beta_R) \in N_- \cup P_- \\ -\pi - (-1)^d \arcsin[(0.5L - R\cos\beta_R)/r_2]\ ; (R,\beta_R) \in N_- \cup P_+ \\ 0\ ; \quad (R,\beta_R) \in S_2 where\ \overline{S_2} is\ the\ \sup\ plementary\ set\ of\ S_2 \end{cases} \quad (36)$$

$$\delta_4 = \begin{cases} (-1)^d \arcsin[(-0.5L - R\cos\beta_R)/r_4]\ ; (R,\beta_R) \in N_+ \cap \overline{S_4} \\ \pi - (-1)^d \arcsin[(-0.5L - R\cos\beta_R)/r_4]\ ; (R,\beta_R) \in N_- \cup Q_- \\ -\pi - (-1)^d \arcsin[(-0.5L - R\cos\beta_R)/r_4]\ ; (R,\beta_R) \in N_- \cup Q_+ \\ 0\ ; \quad (R,\beta_R) \in S_4 where\ \overline{S_4} is\ the\ \sup\ plementary\ set\ of\ S_4 \end{cases} \quad (37)$$

The wheel orientation vector

$$\boldsymbol{\Delta}=(\delta_1,\delta_2,\delta_3,\delta_4)^{\mathrm{T}}\quad \delta_i\in(-\pi,\pi];i=1,2,3,4; \tag{38}$$

The velocity vector

$$\boldsymbol{V}=(\boldsymbol{V}_1,\boldsymbol{V}_2,\boldsymbol{V}_3,\boldsymbol{V}_4)^{\mathrm{T}} \tag{39}$$

$$\boldsymbol{V}_1=\begin{cases}0 & ,(R,\beta_R)\in S_1\\ \boldsymbol{V} & ,(R,\beta_R)\in\{(R,\beta_R)\mid R=\infty\}\\ \boldsymbol{\omega}\times\boldsymbol{r}_1=(-1)^j\omega r_1\,\boldsymbol{k}_0\times\boldsymbol{r}_{10} & ,otherwise\end{cases} \tag{40}$$

$$\boldsymbol{V}_3=\begin{cases}0 & ,(R,\beta_R)\in S_3\\ \boldsymbol{V} & ,(R,\beta_R)\in\{(R,\beta_R)\mid R=\infty\}\\ \boldsymbol{\omega}\times\boldsymbol{r}_3=(-1)^j\omega r_3\,\boldsymbol{k}_0\times\boldsymbol{r}_{30} & ,otherwise\end{cases} \tag{41}$$

$$\boldsymbol{V}_2=\begin{cases}0 & ,(R,\beta_R)\in S_2\\ \boldsymbol{V} & ,(R,\beta_R)\in\{(R,\beta_R)\mid R=\infty\}\\ \boldsymbol{\omega}\times\boldsymbol{r}_2=(-1)^j\omega r_2\,\boldsymbol{k}_0\times\boldsymbol{r}_{20} & ,otherwise\end{cases} \tag{42}$$

$$\boldsymbol{V}_4=\begin{cases}0 & ,(R,\beta_R)\in S_4\\ \boldsymbol{V} & ,(R,\beta_R)\in\{(R,\beta_R)\mid R=\infty\}\\ \boldsymbol{\omega}\times\boldsymbol{r}_4=(-1)^j\omega r_4\,\boldsymbol{k}_0\times\boldsymbol{r}_{40} & ,otherwise\end{cases} \tag{43}$$

$$V_i\in\{V_i\mid V_i\le\min\sqrt{r_i g\mu},V_i\le V_{max};(i=1,2,3,4)\} \tag{44}$$

where the unit vector $\boldsymbol{k}_0$ is perpendicular to the horizontal plane and $\boldsymbol{r}_{i0}\ (i=1,2,3,4)$ is identity vector $\boldsymbol{r}_i\ (i=1,2,3,4)$. The constraint in (44) is the wheel-terrain constraint, where g is gravity acceleration and μ is the frictional coefficients of the wheel-terrain. V_{max} is the maximum scalar quantity of $\boldsymbol{V}_i\ (i=1,2,3,4)$. $\boldsymbol{V}$ is the velocity vector of centre of robot, the rotational velocity around ICR is: $\omega=\begin{cases}V/R & ,R\in\{R\mid 0<R<\infty\}\\ V/p & ,R\in\{R\mid R=0\}\end{cases}$.

We have done the simulations about the algorithm by Matlab7.0 and get the figures on the steering angles vs. R and β_R from Fig.4 and Fig.5: When $\beta_R=\gamma_0,\pi-\gamma_0-\gamma_0,-\pi+\gamma_0$, and $R=p$, $r_i=0$ $(i=1,2,3,4)$, singularity occurs. In our formula, we define $\delta_i=0\ (i=1,2,3,4)$. When $R<p$, the curve of $\delta_i,(i=1,2,3,4)$ is in irregular shape. When $R>p$, the tendency of the curve is regular, when β_R increases, $\delta_i\ (i=1,2,3,4)$ also increase in the range of β_R. The curves of $\delta_i\ (i=1,2,3,4)$ take subsection shape. The tendency of maneuver radius

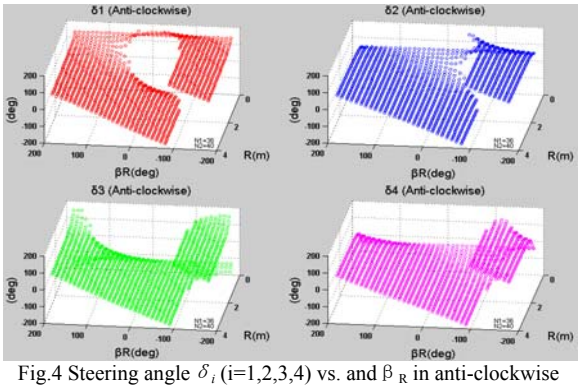

Fig.4 Steering angle δ_i (i=1,2,3,4) vs. and β_R in anti-clockwise

of wheels can be viewed in Fig.6 and the curve takes symmetrical shape to some degree. Further calculation shows that the curves in anti-clock wise are the same to that in clock-wise.

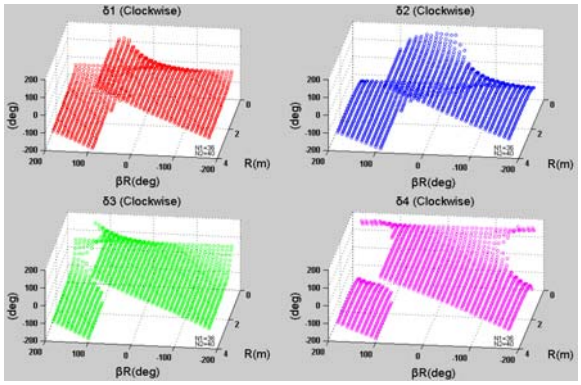

Fig.5 Steering angle δ_i (i=1,2,3,4) vs. R and β_R in clockwise

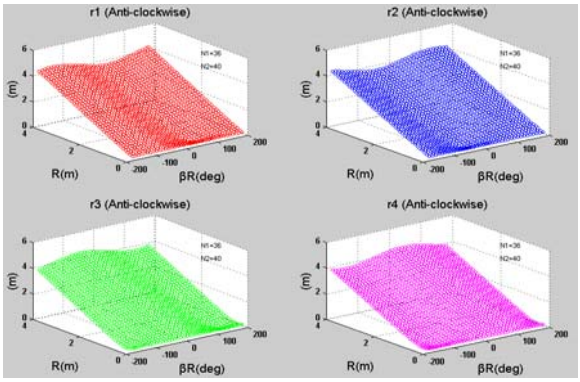

Fig.6 Radius r_i (i=1, 2, 3, 4) vs. R and β_R in anti-clockwise

5 Constrained Maneuver Algorithm

$$\delta_i\in[-\pi/2,\pi/2];i=1,2,3,4; \tag{45}$$
$$R\in[0,\infty),\beta_R\in(-\pi,-\pi]$$

The steering angle of each wheel is as follows:

$$\delta_1=\begin{cases}(-1)^d\arcsin(0.5L-R\cos\beta_R)/r_1\ ;(R,\beta_R)\in M_+\cap\overline{S_1}\\ (-1)^{d+1}\arcsin(0.5L-R\cos\beta_R)/r_1\ ;(R,\beta_R)\in M_-\\ 0;\quad (R,\beta_R)\in S_1\end{cases} \tag{46}$$

$$\delta_3=\begin{cases}(-1)^d\arcsin[(-0.5L-R\cos\beta_R)/r_3]\ ;(R,\beta_R)\in M_+\cap\overline{S_3}\\ (-1)^{d+1}\arcsin[(-0.5L-R\cos\beta_R)/r_3]\ ;(R,\beta_R)\in M_-\\ 0\ ;\quad (R,\beta_R)\in S_3\end{cases} \tag{47}$$

$$\delta_2=\begin{cases}(-1)^d \arcsin[(0.5L-R\cos\beta_R)/r_2]\ ;(R,\beta_R)\in N_+\cap\overline{S_2}\\(-1)^{d+1}\arcsin[(0.5L-R\cos\beta_R)/r_2]\ ;(R,\beta_R)\in N_-\\0\ ;\quad (R,\beta_R)\in S_2\end{cases}\tag{48}$$

$$\delta_4=\begin{cases}(-1)^d \arcsin[(-0.5L-R\cos\beta_R)/r_4]\ ;(R,\beta_R)\in N_+\cap\overline{S_4}\\(-1)^{d+1}\arcsin[(-0.5L-R\cos\beta_R)/r_4]\ ;(R,\beta_R)\in N_-\\0\ ;\quad (R,\beta_R)\in S_4\end{cases}\tag{49}$$

The wheel orientation vector

$$\boldsymbol{\Delta}=(\delta_1,\delta_2,\delta_3,\delta_4)^{\mathrm{T}}\quad \delta_i\in(-\pi,\pi];i=1,2,3,4;\tag{50}$$

The velocity vector

$$\boldsymbol{V}=(\boldsymbol{V}_1,\boldsymbol{V}_2,\boldsymbol{V}_3,\boldsymbol{V}_4)^{\mathrm{T}}\tag{51}$$

$$\boldsymbol{V}_1=\begin{cases}\boldsymbol{\omega}\times\boldsymbol{r}_1=(-1)^d\omega r_1\,\boldsymbol{k}_0\times\boldsymbol{r}_{10};(R,\beta_R)\in M_+\\-\boldsymbol{\omega}\times\boldsymbol{r}_1=(-1)^{d+1}\omega r_1\,\boldsymbol{k}_0\times\boldsymbol{r}_{10};(R,\beta_R)\in M_-\\0\ ;\quad (R,\beta_R)\in S_1\\\boldsymbol{V}\ ;\quad (R,\beta_R)\in\{(R,\beta_R)\mid R=\infty\}\cap M_+\\-\boldsymbol{V}\ ;\quad (R,\beta_R)\in\{(R,\beta_R)\mid R=\infty\}\cap M_-\end{cases}\tag{52}$$

$$\boldsymbol{V}_3=\begin{cases}\boldsymbol{\omega}\times\boldsymbol{r}_3=(-1)^d\omega r_3\,\boldsymbol{k}_0\times\boldsymbol{r}_{30};(R,\beta_R)\in M_+\\-\boldsymbol{\omega}\times\boldsymbol{r}_3=(-1)^d\omega r_3\,\boldsymbol{k}_0\times\boldsymbol{r}_{30};(R,\beta_R)\in M_-\\0\ ;\quad (R,\beta_R)\in S_3\\\boldsymbol{V}\ ;\quad (R,\beta_R)\in\{(R,\beta_R)\mid R=\infty\}\cap M_+\\-\boldsymbol{V}\ ;\quad (R,\beta_R)\in\{(R,\beta_R)\mid R=\infty\}\cap M_-\end{cases}\tag{53}$$

$$\boldsymbol{V}_2=\begin{cases}\boldsymbol{\omega}\times\boldsymbol{r}_2=(-1)^d\omega r_2\,\boldsymbol{k}_0\times\boldsymbol{r}_{20};(R,\beta_R)\in N_+\\-\boldsymbol{\omega}\times\boldsymbol{r}_2=(-1)^{d+1}\omega r_2\,\boldsymbol{k}_0\times\boldsymbol{r}_{20};(R,\beta_R)\in N_-\\0\ ;\quad (R,\beta_R)\in S_2\\\boldsymbol{V}\ ;\quad (R,\beta_R)\in\{(R,\beta_R)\mid R=\infty\}\cap N_+\\-\boldsymbol{V}\ ;\quad (R,\beta_R)\in\{(R,\beta_R)\mid R=\infty\}\cap N_-\end{cases}\tag{54}$$

$$\boldsymbol{V}_4=\begin{cases}\boldsymbol{\omega}\times\boldsymbol{r}_4=(-1)^d\omega r_4\,\boldsymbol{k}_0\times\boldsymbol{r}_{40};(R,\beta_R)\in N_+\\-\boldsymbol{\omega}\times\boldsymbol{r}_4=(-1)^d\omega r_4\,\boldsymbol{k}_0\times\boldsymbol{r}_{40};(R,\beta_R)\in N_-\\0\ ;\quad (R,\beta_R)\in S_4\\\boldsymbol{V}\ ;\quad (R,\beta_R)\in\{(R,\beta_R)\mid R=\infty\}\cap N_+\\-\boldsymbol{V}\ ;\quad (R,\beta_R)\in\{(R,\beta_R)\mid R=\infty\}\cap N_-\end{cases}\tag{55}$$

$$V_i\in\{V_i\mid V_i\le\min\sqrt{r_i g\mu},V_i\le V_{max};\ (i=1,2,3,4)\}\tag{56}$$

The radius of wheel is given in (30) to (33).

The results of simulations on the algorithm by Matlab7.0 are in the Fig.7 and Fig.8:

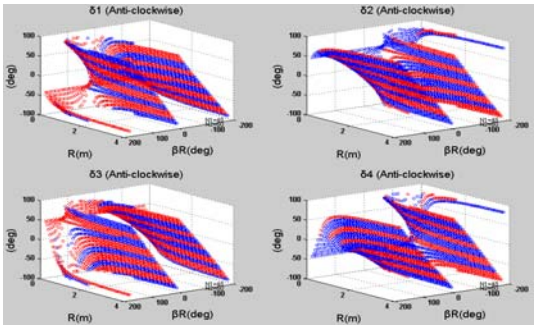

Fig.7 Steering angle δ_i (i=1,2,3,4) vs. R and β_R in anti-clockwise

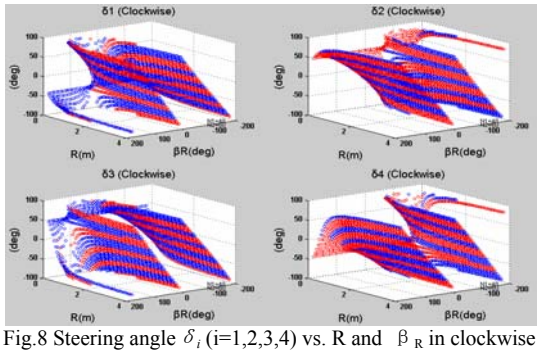

Fig.8 Steering angle δ_i (i=1,2,3,4) vs. R and β_R in clockwise

In this algorithm, $\delta_i\in[-\pi/2,\pi/2];\ i=1,2,3,4$ ..

The singularity is as the same situation in section 4. We can see that the velocity of the driven wheel area (in blue colour) and the inversed velocity of driven wheel area (in red colour) distribute by interlacement, and these distributions are just opposite in the figure of the anti-clockwise rotation and clockwise rotation. To a certain value of *R*, when β_R increases, $\delta_i=0;\ i=1,2,3,4$ also increases. The radii distribution is relative to the rotational direction. The tendency of maneuver radius of wheels can be viewed in Fig.9 and the curve takes symmetrical shape to some degree. Further calculation shows that the curves in anti-clock wise are the same to that in clock-wise.

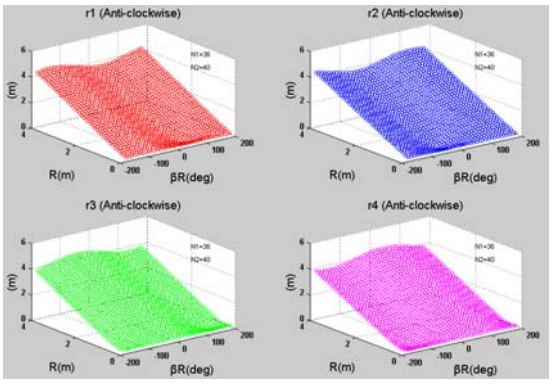

Fig.9 Maneuver radius r_i (i=1, 2, 3, 4) vs. R and β_R in

6 Test Validation

Tests for different type of maneuver modes have been implemented. Fig.10 is for Ackerman mode, Fig.11 is for Double-Ackerman mode, Fig.12 if for the test of robot rotating around the point where the

wheel 4 contacts the ground, Fig.13 is for the test of robot rotating around the point located within supporting area, Fig.14 is for the test of robot rotating around the point locates at the rear exterior supporting area, Fig.15 is for the test of robot rotating around the point locates at the sharp rear exterior supporting area and Fig.16 is for the test of robot rotating around the point located at the sharp front of exterior supporting area.

Fig.10 Test of robot on Ackerman maneuver mode

Fig.11 Test of robot on Double-Ackerman maneuver mode

Fig.12 Test of robot rotates around the point where wheel 4 contacts with ground

Fig.13 Test of robot rotates around the point which locates within supporting area

Fig.14 Test of robot rotates around the point locates at the rear exterior supporting area

Fig.15 Test of robot rotates around the point locates at the sharp rear exterior supporting area

A criterion z_p which is called the ICR superposition rate is defined to describe the positional precision of center of trajectory circle of robot compared with ideal ICR position.

$$z_p = (1 - \frac{\text{positional windage of trajectory circle } \Delta p}{\text{radii of trajectory circle } R_t}) \times 100\%$$

Table 2. Test Results of Maneuver Motion of Mobile Robot

No	(R, β_R) (cm),(deg)	Δp	z_p	Max z_p	Min z_p	Ave. z_p
1	(73.3,-110.7)	1.1	98.49	98.4	97.81	98.1
		1.3	98.22			
		1.5	97.95			
		1.6	97.81			
2	(1 (50.0,-90.0)	4.8	98.6	96.9	96.60	96.7
		5.0	96.66			
		5.1	96.60			
		4.6	96.93			
3	(39.5,-131.4)	0.5	98.73	98.9	97.46	98.2
		0.4	98.98			
		1.0	97.46			
		0.8	97.97			
4	(19.6,-131.4)	0.3	98.46	98.9	96.93	98.1
		0.2	98.97			
		0.6	96.93			
		0.4	97.95			
5	(50,-170)	1..2	97.60	97.8	97.20	97.5
		1..3	97.40			
		1.1	97.80			
		1.4	97.20			
6	(150,-180)	4..9	96.73	96.8	96.60	96.7
		4.7	96.86			
		4.8	96.80			
		5.1	96.60			

As in Table 2, the average of z_p takes decrease tendency with the radii of trajectory of robot R_t, this result shows that the windage of the steering angle of wheels will cause biggish errors. The ICR superposition rate is great than 90%.

7 Conclusion and Future Works

A general description about the maneuverability of robot on plane is derived. The motion of a robot with 4WS4WD on a plane under the kinematical constraints can be described as a rotation motion around ICR and a translation motion (in this case, the ICR can be regarded as being at infinity). The proof of existence of ICR has been given. A generic maneuver algorithm around the ICR has been developed, and the singularity has been analyzed. This algorithm has the advantage of continuous wheel steering motion. Another generic maneuver algorithm with the range constraints of steered wheels based on ICR has been developed. And the singularity has been analyzed. This algorithm has the advantage of high efficiency and lower energy-consumption. A wheel-terrain constraint has been presented in the velocity control to ensure implementation of the two algorithms. Tests for robot rotating around different position of ICR have been implemented to verify these algorithms.

Our future works include research on the error analysis on the maneuver mode.

References:

[1] B.C.Besselink, "Computer control steering system for vehicles having two independently driven wheels," *Computer and Electronics in Aagriculture*, vol. 39, pp.219-226, 2003.

[2] Thoms Bak, Hans Jakobsen, "Agriculture Robotic Platform with Four Steering for Weed Detection," Biosystems Engineering, vo87, no2, pp.125-136, 2004.

[3] Thoms Bak, Jan Bendtsen, Anders P. Ravn, "Hybrid Control Design for a Wheeled Mobile Robot," Berkeley University Web Site (November 1, 2004). [On-line]. Available: www.eecs.berkeley.edu/

[4] Roland Siegwart, Illah R. Nourbrakhsh, Introduction to Autonomous Mobile Robot, London: The MIT Press, 2004, pp.67-68.

[5] Tarokh M, McDermot G, Hayati S, Hung J. Kinematic modeling of a high mobility Mars rover. Proceedings of the 1999 IEEE International Conference on Robotics & Automation, Detroit, Michigan,1999,: pp.992-998